JAARGANG 27 NUMMER 3 SEPTEMBER 2023

GEO kunst

ONAFHANKELIJK VAKBLAD VOOR GEBRUIKERS VAN GEOKUNSTSTOFFEN

XII ICG

NGO IGS Netherlands

12TH ICG – ROME ITALY
INTERNATIONAL CONFERENCE ON GEOSYNTHETICS
GEOSYNTHETICS: LEADING THE WAY TO A RESILIENT PLANET

GEOKUNST WORDT MEDE MOGELIJK GEMAAKT DOOR:

HOOFD-SPONSORS

Bestuur 'Nederlandse Geotextiel Organisatie' (NGO - IGS Netherlands):
Erik Kwast, Rijk Gerritsen, Iljo Fluit, Suzanne van Eekelen, Leo Kuljanski, Joris van den Berg. Technisch secretaris Joop Groenveld.

DE GEZAMENLIJKE LEDEN VAN DE NGO ZIJN:

CDR International BV, Rijssen
Cofra B.V., Amsterdam
Deltares, Delft
Enviro Quality Control BV, Maarssen

Fugro NL Land B.V., Leidschendam
Geonius, Geleen

GID Milieutechniek, Velddriel
Havenbedrijf Rotterdam
Huesker Synthetic BV, Rosmalen

Juta Holland BV, Oldenmarkt
Kiwa NV, Rijswijk
Kwast Consult, Houten
Movares Nederland BV, Utrecht

Normec QS, Bennekom
Robusta BV, Genemuiden
Rijkswaterstaat, Utrecht

Tefab B.V., Gilze

Witteveen + Bos, Deventer

VOORWOORD

BESTE LEZERS,

Geosynthetics: Leading the Way to a Resilient Planet. Dit is het thema van de 12th International Conference on Geosynthetics (12th ICG). Het congres vindt plaats van 17 t/m 21 september 2023 in Rome in Italië. Ten behoeve van het congres heeft de Nederlandse Geotextiel Organisatie (NGO) een congres special uitgebracht (GeoArt) en deze wordt overhandigd aan alle 800-1000 congres deelnemers. In dit nummer van Geokunst zijn de drie Engelstalige artikelen opnieuw gepubliceerd.
De Nederlandse Geotextiel Organisatie (NGO, de officiële Nederlandse afdeling van de IGS), is onze Italiaanse collega's enorm dankbaar voor de intensieve voorbereiding van deze conferentie.

De 12th ICG is het meest toonaangevende en grootste internationale evenement voor geokunststoffen. De conferentie brengt alle internationale experts in de geokunststoffen branche samen. En een intensief 4-daags programma vol met keynote lezingen, trainingssessies, paper presentaties, werkgroep vergaderingen, een IGS jaarbijeenkomst en een grote tentoonstelling met deskundige bedrijven. Daarnaast zijn er talloze gelegenheden om met elkaar in contact te komen, te leren en geïnspireerd te worden.

Werken aan een veerkrachtige planeet en samenleving is absoluut noodzakelijk. De effecten van klimaatverandering zijn dagelijks in het nieuws, met toenemende periodes van extreme droogte, zware regenval en een stijgende zeespiegel. Deze factoren hebben nu al gevolgen voor miljoenen mensen en waarschijnlijk zullen de gevolgen de komende jaren alleen maar toenemen. Eén van de belangrijkste doelstellingen van de EU Green Deal[1)] en nationale programma's is om de CO_2-uitstoot aanzienlijk te verminderen (mitigatie). Het goede nieuws is dat met het gebruik van geokunststof toepassingen de CO_2 uitstoot beperkt kan worden. Dit biedt aanzienlijke kansen voor civiele, waterbouwkundige en milieutechnische sectoren. Zo kan met een gewapende grondconstructie de CO_2-uitstoot gemiddeld 75% (!) verminderen in vergelijking met een traditionele oplossing met een stalen damwand. Een ander cruciaal aspect binnen het conferentiethema is klimaatadaptatie: het creëren van veerkrachtige oplossingen ten behoeve van veranderende omstandigheden als gevolg van klimaatverandering. Geokunststoffen kunnen bijdragen aan het creëren van dergelijke klimaat-adaptieve en duurzame oplossingen. Hierbij kan gedacht worden aan het verbeteren van waterkeringen, kustbescherming, duurzame infrastructuuroplossingen, wateropvangsystemen voor extreme regenval en wateropslag voor periodes van intense droogte.

In dit GeoKunst magazine vinden jullie drie interessante artikelen met Nederlandse kennis en ervaringen, die de toegevoegde waarde van geokunststoffen benadrukken. Het eerste artikel presenteert een richtlijn voor een deels onder water staande met geotextiel versterkte paalmatras ophoging. Het tweede artikel beschrijft de klimaatuitdagingen en de rol van geokunststoffen bij het verbeteren van waterkeringen en kustbescherming. Het derde artikel presenteert tenslotte kleinschalige geocentrifuge-experimenten met geogrid-verankerde damwanden.

Wij worden allemaal geconfronteerd met meerdere en steeds grotere uitdagingen als gevolg van de klimaatverandering. De tijd tikt door. We hebben weinig tijd om grote stappen voorwaarts te maken en geokunststoffen deel te laten uitmaken van onze duurzame toekomst. Wie gaat de uitdaging aan?

Ik wens jullie veel leesplezier. *Be smart. Be resilient.*

Rijk Gerritsen
Eindredacteur Geokunst

1) https://commission.europa.eu/strategy-and-policy/priorities-2019-2024/european-green-deal_en

COLOFON

Geokunst wordt uitgegeven door de Nederlandse Geotextiel Organisatie (NGO). Het vaktijdschrift verschijnt vier keer per jaar en wordt toegezonden aan abonnees of op verzoek. De NGO is de officiële Nederlandse afdeling van de International Geotextile Society (IGS). De NGO is een vereniging zonder winstoogmerk bestaande uit kennisinstituten, laboratoria, inspectie- en certificatieinstellingen, ingenieursbureaus, aannemers, overheidsinstanties, producenten en leveranciers. De NGO stimuleert kennis over duurzaam ontwerpen, verantwoord gebruik en bouwen met hoogwaardige geokunststoffen met vele toepassingen in de civiele techniek, waterbouw, milieu en bouw.

Eindredactie **Rijk Gerritsen**
Tekstredactie **Jurjen van Deen**
Redactieraad **Adam Bezuijen, Piet van Duijnen, Suzanne van Eekelen, Paul ter Horst, Tara van der Peet**
Productie **Uitgeverij Educom**

Een abonnement kan worden aangevraagd bij:
Nederlandse Geotextielorganisatie (NGO)
info@ngo.nl **www.ngo.nl**


S.J.M. van Eekelen
Deltares,
The Netherlands


R.A. Zwaan
Deltares,
The Netherlands


A. Nancey
Solmax / TenCate
Geosynthetics,
France


M. Hazenkamp
Solmax / TenCate
Geosynthetics,
The Netherlands


Y. H. Jung
Kyung Hee University,
Republic of Korea

FOUR YEARS FIELD MEASUREMENTS IN A PARTLY SUBMERGED WOVEN GEOTEXTILE-REINFORCED PILE-SUPPORTED EMBANKMENT

Introduction

The design guideline CUR226:2016 for geosynthetic-reinforced pile-supported (GRPS) embankments adopted the Concentric Arches (CA) model of van Eekelen (2013, 2015), which was validated with more than 100 measurements taken in the field and in experiments. These embankments were all reinforced with at least one layer of geogrid. Furthermore, all the embankments were unsaturated, and installed above the groundwater table.

Limited research was done on the influence of water in a piled embankment. Briançon and Simon (2012), Sloan (2011), and van Eekelen et al. (2020) showed that heavy rainfall affects measurements. Song et al. (2018) concluded from 2D trapdoor tests with sand that groundwater can degrade the soil arching mechanism. Wang et al. (2019), however, found strengthening of soil arching with increasing water level in full-scale 3D model experiments.

The validated use of CUR226:2016 is possible for geometries, conditions and materials that match the situation where the measurements for the validation were taken. If these requirements are not met, the guideline requests additional measurements to demonstrate that the CA model gives good results for these conditions, too.

For this purpose, field measurements were done in a partly submerged piled embankment, reinforced with geotextiles only, without geogrids. This paper compares the measured strains with the varying groundwater table and air temperature, and calculations with the CA model of CUR226:2016. This paper is a modified version of van Eekelen et al. (2023).

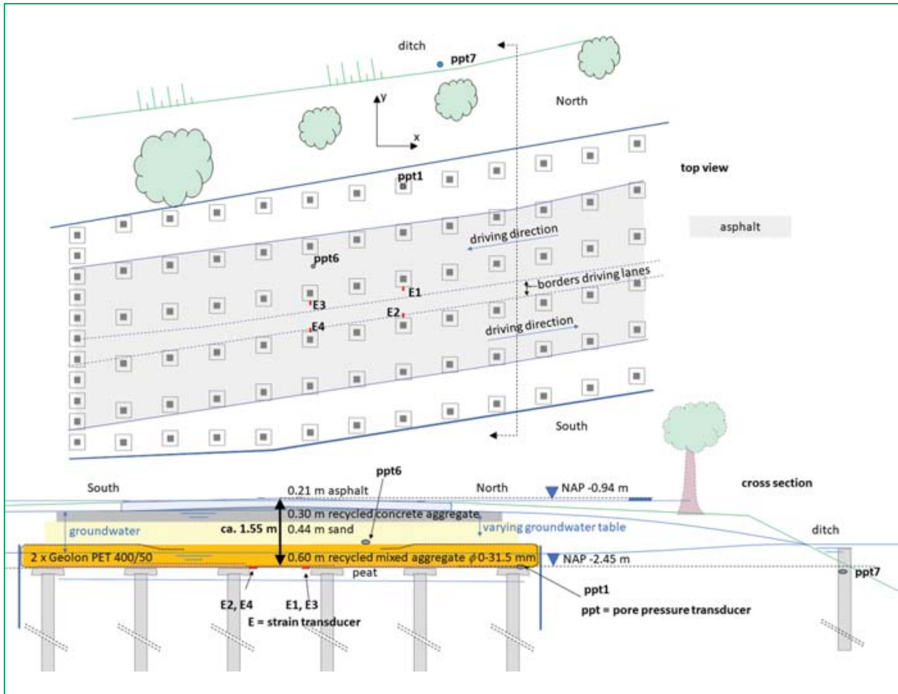

Figure 1 – Lay-out of the geotextile-reinforced piled embankment and the monitoring equipment.

A partly submerged geotextile-reinforced piled embankment

Van Eekelen et al. (2022) describe a piled embankment in the Netherlands for a regional motor way that was opened on 6 April 2019. Pile caps (0.75 m x 0.75 m), with smooth, rounded edges, were installed on end-bearing prefab concrete piles with an average centre-to-centre spacing of 2.28 m x 2.27 m. Two layers of woven geotextile (TenCate Geolon® PET 400/50) were installed, one with the machine (strong) direction across the road axis, the second parallel to the road axis. Figure 1 shows part of the monitoring set-up. In addition, the air temperature was measured hourly. For more details of the experimental set-up, we refer the reader to van Eekelen et al (2023).

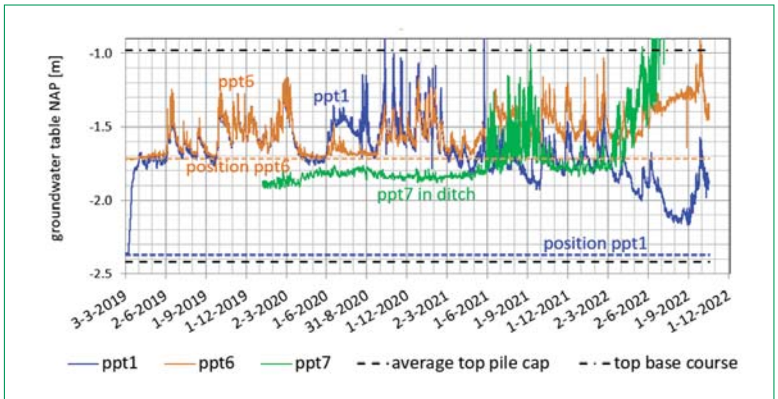

Figure 2 – Measured pore pressures, translated into groundwater table (ppt1 and ppt6) and ditch water table (ppt7).

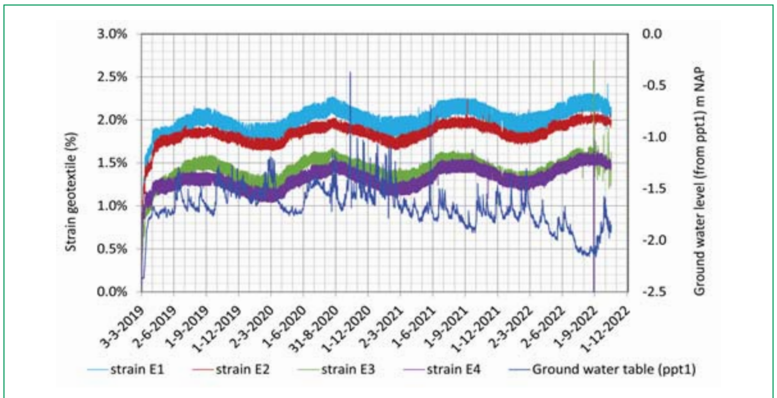

Figure 3 – Comparison measured geotextile strains and to measured groundwater table (ppt1).

ABSTRACT

This paper describes measurements in a partly submerged piled embankment, reinforced with geotextiles only. The seasonal effect in the measured geotextile strains strongly matches the seasonal temperature variation. No correlation with the varying groundwater table was found. The measurements remain sufficiently on the safe side of the results of the Concentric Arches model. Therefore, the CUR226:2016 design guideline may be used for this type of geotextile-reinforced pile-supported embankments, of which the embankment is installed partly below the groundwater table.

Measurements

PORE PRESSURES AND GROUNDWATER TABLE

Figure 2 shows the measured pore pressures, translated into groundwater level in m NAP, where NAP is the Dutch reference level. The figure indicates the positions of ppt1 and ppt6; ppt1 lies in saturated soil. However, ppt6 is located higher, and the groundwater table sometimes drops below ppt6.

Figure 2 shows what can happen if a pore pressure transducer is installed in unsaturated soil. Until June 2020, ppt1 and pp6 match. Just before 1 June 2020, the groundwater table drops below ppt6. This causes an air bubble that starts disturbing the measurements of ppt6, keeping the values of ppt6 well below those of ppt1. In September 2020, the groundwater level passes ppt6 again, the air bubble disappears, and ppt1 and ppt6 match again. In April 2021, the groundwater table passes ppt6 again, resulting in another air bubble that makes the measurements of ppt6 unreliable again.

It seems plausible that ppt1 continuously gives reliable results; it shows a low water table during the very dry summer of 2022, followed by a rainy period in September 2022. The pore pressure transducer in the ditch gave reliable results between February 2020 and June 2021 and between November 2021 and March 2022.

GEOTEXTILE STRAINS COMPARED TO GROUNDWATER TABLE AND AVERAGE DAY AIR TEMPERATURE

Strain gauges E1 and E2 give higher values than strain gauges E3 and E4 (Figure 3). We cannot explain this difference. The strains show a sea-sonal effect; the strains are higher during summers than during winters. Furthermore, each summer gives slightly higher strains than the previous summer. This can be explained by the creeping behaviour of the geotextile. The measured strains do not correlate clearly with the ground-water table.

Figure 4 zooms in on four dry weeks and four wet weeks. The figure shows a clear daily cycle, the cause of which is unclear. A similar daily effect was found earlier by van Eekelen et al. (2007). The daily cycles of traffic load or soil temperature may have an influence. However, the different strain gauges do not show a peak at the same time of the day.

Figure 4b shows an immediate response on rain: the daily cycle is less clear. Possibly, the relatively constant and low temperature caused by the rain flattens the daily cycle.

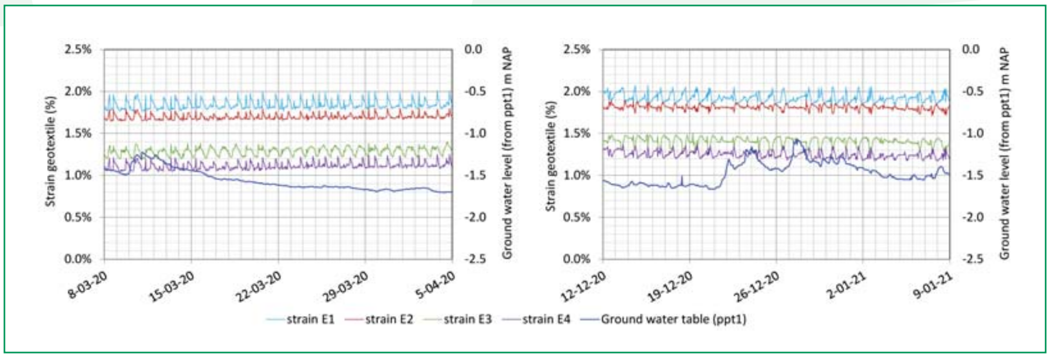

Figure 4 – Two four-week details of Figure 3; measured geotextile strains and measured groundwater table (a) dry period (no rain) and (b) wet period (several rainy periods).

Table 1 – Parameters used for the calculations with the Concentric Arches model*

Date	2019					2020	2030
	28 Feb	1 Mar	5 Mar	12 Mar	24 Apr	29 Feb	25 Aug
Height fill (m)	0.00	0.30	0.60	1.00	1.51	1.51	1.51
Tensile stiffness geotextile (kN/m)	3200	3200	3200	2961	2722	2544	2426

*Other input values: centre-to-centre distance piles s_x = 2.27 m, s_y = 2.28 m, square pile caps width a = 0.75 m, unit weight fill γ = 19 kN/m³, fill friction angle fill φ = 34° and 38°, subgrade reaction k = 0 kN/m³, traffic load p = 0 kPa and 11.5 kPa (25% of the design load), soil arching reduction coefficient κ is either 1.0 (no soil arching reduction) or 1.58 (soil arching reduction).

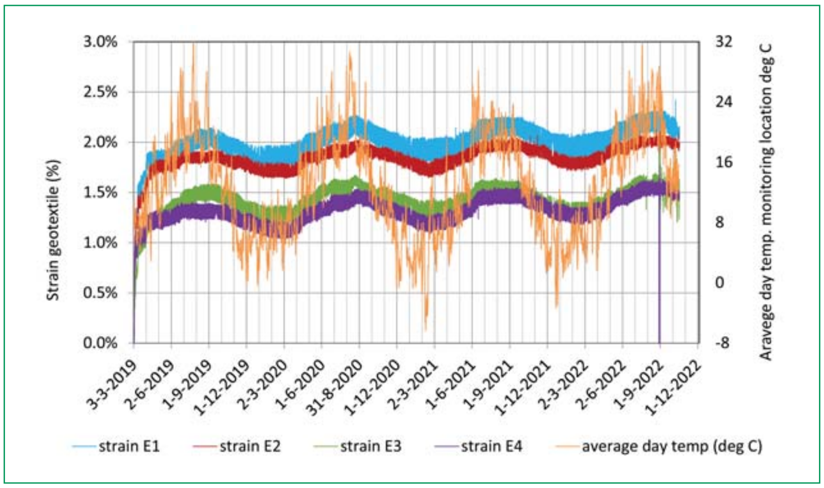

Figure 5 – Comparison measured geotextile strains and the day-average of the air temperature which was measured hourly at the field monitoring location.

Figure 5 shows that the seasonal cycle of average day temperature clearly correlates with the geo-textile strains. The geotextile strains are higher in summer. The thermal expansion of the road surface is too small to play a significant role in this seasonal cycle.

Calculations with the Concentric Arches model

The geotextile strains were calculated using the CA model (van Eekelen, 2013, 2015, CUR226: 2016). No partial factors were used. Table 1 gives the input parameters. Some remarks:

- Usually, the traffic load is chosen p = 0 kPa when comparing the model results to field measure-ments. In addition to that, a calculation was performed with 25% of the design load, to account for the permanent influence of the traffic load on the strains in the geotextile.
- CUR226:2016 requests to reduce the soil ar-ching for a relatively thin piled embankment like this one, with a high traffic load. It is assu-med that the soil arching is reduced perma-nently due to the on-going traffic load. The soil arching reduction factor (κ) equals 1.58 for this configuration and traffic load, following Table

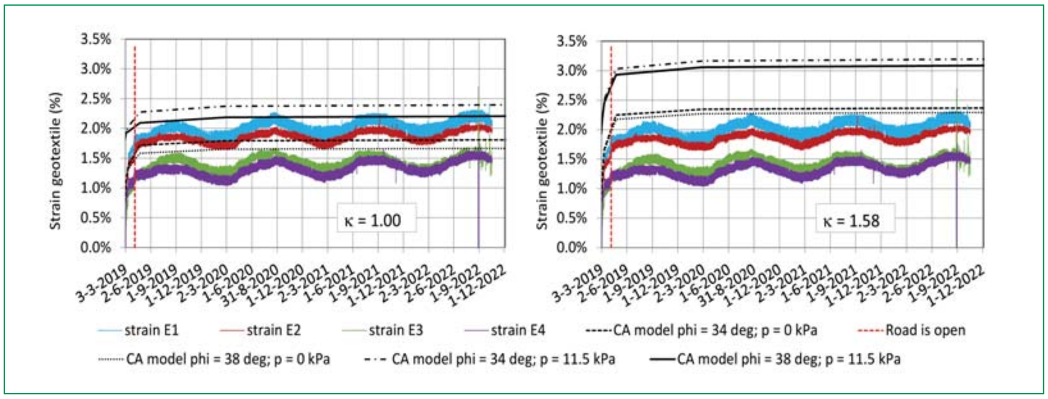

Figure 6 – Comparison measured geotextile strains and geotextile strains calculated with the CA model. Predictions higher than measured values are on the safe side.

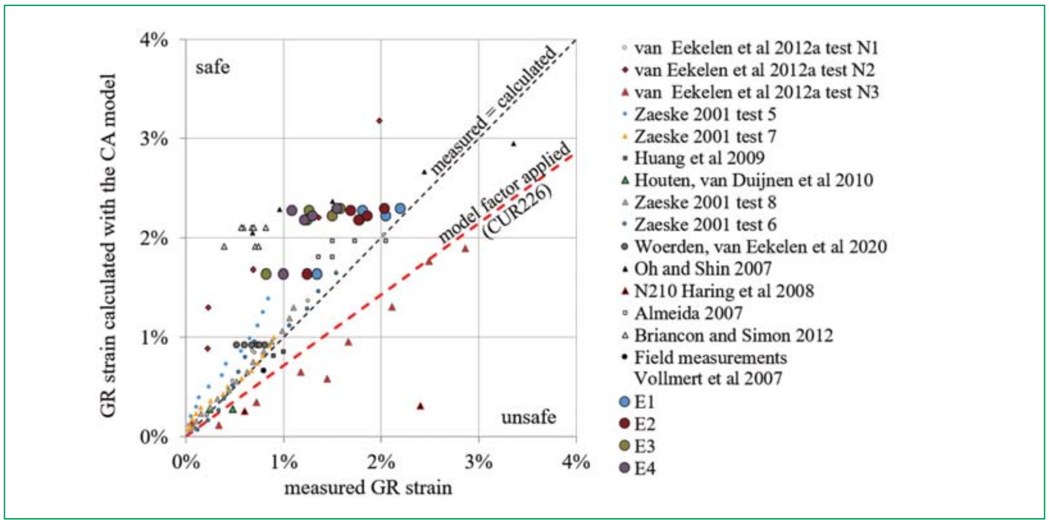

Figure 7 – Extension of the validation of the CA model with the new data, with in the calculations: φ = 38º, traffic load p = 0 kPa and K = 1.58. Measured values of E1, E2, E3, E4 are day averages on 12-3 / 24-4 / 1-9-2019 and 29-2 /1-9-2022. The calculations were done using the input values given in Table 1.

2.3 of CUR226:2016.

– It is expected that the calculation with some traffic load and soil arching reduction matches the real situation best.

Comparisons measurements and calculations

Figure 6 compares the measured and calculated geotextile strains. The smallest calculated strains agree reasonably well with the average values of E1 - E4. All other calculations give higher values than the measured values, so application of CUR226:2016 leads to a safe design.

Figure 7 extends of the validation of van Eekelen et al. (2015). The figure shows that the measurements of E1 and E2 agree well with the calculations, and the measurements of E3 and E4 give lower values than calculated. This result is on the safe side, too. From this, we may conclude that the CA model, and therefore CUR226:2016, is applicable for this piled embankment of which the embankment was installed partly below the groundwater table. This conclusion is valid for woven geotextiles as applied in this monitoring project.

Conclusions

A partly submerged geotextile-reinforced piled embankment was monitored. The measured geotextile strains show no correlation with the groundwater level. However, the measured strains have a strong seasonal cycle that match the seasonal cycle in the average day air temperature quite well. This seasonal relationship between the air temperature and the geotextile strains should be further analysed.

The CA model matches the measurements well. The CUR226:2016 design guideline adopted this CA model. Therefore, CUR226:2016 is applicable for this type of geotextile-reinforced piled embankment, which is installed partly below the groundwater table. This conclusion is valid for the woven geotextiles as applied in this monitoring project.

Acknowledgements

The authors are grateful for the support of the TKI-PPS funding of the Dutch Ministry of Economic Affairs, TenCate Geosynthetics, the Kyung Hee University in Seoul, Republic of Korea, BAM and Deltares, Netherlands.

References

– Briançon, L., Simon, B. 2012. Performance of Pile-Supported Embankment over Soft Soil: Full-Scale Experiment. Journal of Geotechnical and Geoenvironmental Engineering 138, 551–561. BSI 2015.
– CUR226:2016. van Eekelen S.J.M. & Brugman, M.H.A. (Eds.) 2016. Design Guideline Basal Reinforced Piled Embankments. CRC Press, Delft, Netherlands.
– Sloan, J.A. 2011. Column-Supported Embankments: Full-Scale Tests and Design Recommendations. PhD Thesis. Virginia Polytechnic Institute and State University, Blacksburg, Virginia, USA.
– Song, J., Chen, K., Li, P., Zhang, Y. & Sun, C. 2018. Soil arching in unsaturated soil with different water table. Granular Matter 20, 78.
– van Eekelen S.J.M. 2015. Basal Reinforced Piled Embankments. PhD Thesis Delft University of Technology, Delft, Netherlands. ISBN 978 94 6203 825 7.
– van Eekelen, S.J.M., Van, M.A. Bezuijen, A. 2007. The Kyoto Road, a full-scale test. Measurements and calculations. In: Proceedings of ECSMGE14, Madrid, Spain 1533-1538.
– van Eekelen S.J.M., Bezuijen, A., van Tol, A.F. 2013. An analytical model for arching in piled embankments. Geotextiles and Geomembranes 39, 78–102.
– van Eekelen S.J.M., Bezuijen, A. van Tol, A.F. 2015. Validation of analytical models for the design of basal reinforced piled embankments. Geotextiles and Geomembranes 43, 56–81.
– van Eekelen, S.J.M., Bezuijen, A., van Duijnen, P.G., 2012. Does a piled embankment 'feel' te passage of a heavy truck? Field measurements. In: Proc. 5th European Geosynthetics Congress, Valencia, Spain, pp 162-166.
– van Eekelen S.J.M., Venmans, A.A.M., Bezuijen, A. van Tol, A.F. 2020. Long term measurements in the Woerden geosynthetic-reinforced pile-supported embankment. Geosynthetics Int. 27-2, 142-156.
– van Eekelen, S.J.M., Zwaan, R., Nancey, A., Hazekamp, M., Jung, Y.M. 2022. Field measurements in a partly submerged woven geotextile-reinforced pile-supported embankment. Proc. EuroGeo7, Poland. IOP Conf. Ser.: Mater. Sci.vEng. 1260 012046. doi:10.1088/1757-899X/1260/1/012046.
– van Eekelen, S.J.M., Zwaan, R., Nancey, A., Hazekamp, M., Jung, Y.M. 2023. Four years field measurements in a partly submerged woven geotextile-reinforced pile-supported embankment. Proc. ICG12, Rome, Italy.
– Wang, H.L., Chen, R.P., Cheng, W., Qi, S. & Cui, Y.J. 2018. Full-scale model study on variations of soil stress in geosynthetic-reinforced pile-supported track bed with water level change and cyclic loading. Can. Geotech. J. 56: 60–68 (2019).


TENCATE
Geolon® HMi
ALLES-IN-ÉÉN OPLOSSING:
STERKE KWALITEIT DIE JE ZIET!
Een onmiskenbaar design gecombineerd
met de hoogste technische prestaties
Tel: + 31 (0)546 544 811
nederland@tencategeo.com
www.tencategeo.eu
TENCATE
GEOSYNTHETICS
A Solmax
Company


Naue
Duurzame grond, weg en waterbouw projecten
Innovatieve oplossingen met hoogwaardige geo-bouwmaterialen
• Talrijke toepassingen en voordelen van geo-bouwmaterialen in grond, weg en waterbouw projecten, als infrastructuur en waterkeringen.
• Innovatieve en duurzame oplossingen met bentonietmatten, folieconstructies, geogrids, (gewapende grond, funderingswapening), erosie- en drainagematten, filter- en scheidingsdoeken.
• Beproefde oplossingen die aangepast kunnen worden naar uitdagende omstandigheden ter plaatse.
• Ondersteuning vanaf de eerste haalbaarheid, het ontwerp met berekeningen en tekeningen, levering materialen én installatie.
Naue Prosé
Geotechniek B.V.
Postbus 564
8901 BJ Leeuwarden
netherlands@naue.com
Building on sustainable ground.
naue.com

R.H. Gerritsen
Naue Prosé Geotechniek B.V., The Netherlands

A. Bezuijen
University Ghent, Belgium / Deltares Delft, The Netherlands

C. Dorst
Dowaco, The Netherlands

CLIMATE CHANGE AND EXTREME WEATHER CONDITIONS: THE ROLE OF GEOSYNTHETICS SECURING FLOOD DEFENCES AND COASTAL PROTECTION

Introduction

Climate change has brought rapidly changing hydraulic conditions, with heavier rainfall, more severe storms, higher river discharges, increased flow velocities and wave overtopping. With nearly a billion people living in low-lying areas near rivers and coastlines, securing and improving flood defences and flood protection schemes has become a global challenge. Integrating geosynthetics on a larger scale into designs can lead to better, faster and/or cheaper construction of new flood defences, levee reinforcements or coastal protections. This has the potential to considerably boost global flood protection programs. This paper illustrates the benefits and added value of applying geosynthetics in flood defences, aiming to encourage the use of these materials by designers, contractors and authorities. This paper is a shorter and modified version of Gerritsen et al. (2023).

Climate change observations and impact

Based on data, global sea levels have risen about 0.20 m during the last 100 years, and the rate of rise is accelerating. The implications and consequences of the rising sea levels for people on earth are enormous. The Intergovernmental Panel on Climate Change (IPCC, 2022) has made global assessments of potential scenarios, that predict a sea level rise between 0.3 m and 1.5 m by 2150, depending on the climate scenario. Figure 1 combines measurements and predictions of sea level rise, clearly illustrating the major challenges in reinforcing existing, or realising new flood defences.

The predictions of sea level rise obviously contain uncertainties; nevertheless, the values will have significant implications for the safety, liveability and sustainability of residential, commercial and agricultural areas. Effects such as dune and beach erosion along coastlines, due to high-water conditions, will become increasingly frequent and intense.

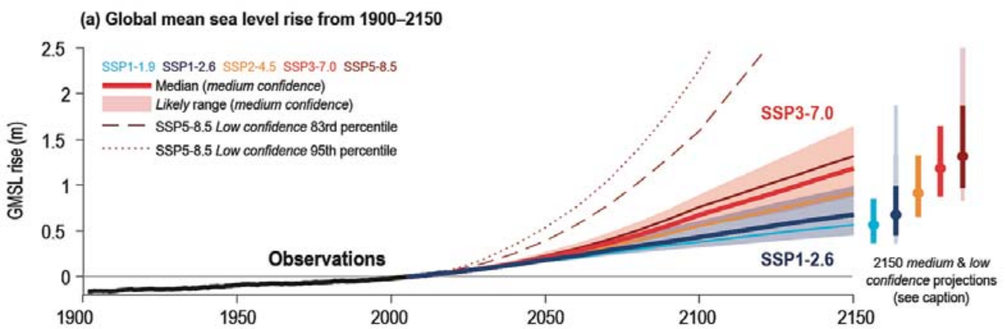

Figure 1 – Projected Global Mean Sea Level Rise (1950-2150) under different SSP scenarios, given in different colours and reliability range by IPCC (2022), Box TS.4 Sea Level, Figure adapted by Deltares.

The global damage costs that result from floods due to sea level rise are expected to increase significantly. Jevrejeva et al. (2018) show that with a 0.86 m sea level rise (RCP8.5 scenario, median value) and without additional measures for flood defences, the worldwide estimated flood damage costs in the year 2100 are 11600 billion euro/year. However, implementing measures to improve coastal protection, could potentially reduce these annual costs by about a factor 10. Despite this reduction, the costs remain substantial, indicating that the impact of sea level rise and consequential costs of flooding will be very high for all coastal areas worldwide.

Haasnoot et al. (2018) listed possible measures for adaption to the accelerated sea level rise in the Netherlands.

1. Higher and wider flood defences;
2. More beach nourishment;
3. Structural measures to maintain the fresh water supply and water safety;
4. Considerably higher frequencies in closing storm surge barriers.

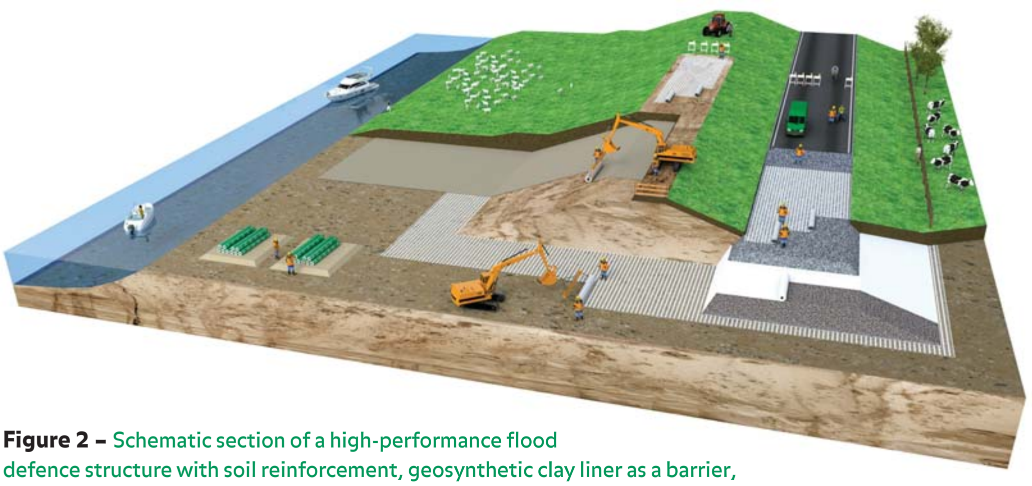

Figure 2 – Schematic section of a high-performance flood defence structure with soil reinforcement, geosynthetic clay liner as a barrier, nonwoven geotextile for filtration and separation and erosion control products on the embankments. Other possibilities (not shown) are erosion control mats and filter layers below a stone revetment.

Applying geosynthetics can have a significant potential for adaptation measures. In this paper we will focus on applications in flood defence structures (1) and coastal defence (2). Building with geosynthetics is highly sustainable, enables the use of local less suitable soils and building in difficult circumstances.

ABSTRACT

In the coming decades, it will be a great challenge to respond effectively to the global climate change, causing sea level rise, heavy rainfall, storms and extreme droughts. This response involves both climate mitigation, through CO_2 reduction, and climate adaption, which requires adjusting our physical surroundings to the changed environmental conditions. Geosynthetics can play a significant role in addressing these challenges. Geosynthetics contribute to CO_2 reduction, thereby limiting climate change. Additionally, applying geosynthetics in flood defences mitigates issues like higher hydraulic loads, erosion and stability concerns. This paper describes some valuable applications of geosynthetics for adapting and creating safe and resilient living areas.

Geosynthetics for flood defences

Geosynthetics can serve various functions in flood defences, like erosion protection, reinforcement, separation, sealing, drainage and filtration. Their potential contribution to levee reinforcements is considerable (Gerritsen et al., 2019). However, the complexity of levee reinforcements becomes larger due to higher safety requirements, the need to preserve landscape and buildings, and more severe hydraulic conditions. Also financial budgets for flood control are under pressure. Consequently, alternative and innovative techniques are increasingly seen as necessary or highly desirable.

Figure 2 shows a cross section of a flood defence structure, showing multiple geosynthetics for various functions. Geosynthetic applications reduce the use of primary soil building materials, enables the use of locally available soil, and significantly minimises the environmental impact through lower CO_2 emissions compared to traditional building methods.

To ensure adequate flood defences in the future, the frequency of levee reinforcements in the coming decades will increase. It is therefore important to design the structures in a way that allows for easy adaptation during the next levee reinforcement. This involves ensuring that (geo-synthetic) materials can be easily removed from the ground or that structures are extendable.

GEOTEXTILE FILTER CONSTRUCTIONS UNDER STONE REVETMENTS

Stone revetments play an important role in protecting levees and coastlines. The selection of stone gradings, ranging from 10 kg to over 3 tonnes, depends on the hydraulic conditions. To ensure their proper functioning, it is essential to apply an adequate filter layer system that prevents gradings or subsoil to be washed away. Traditional filtersystems can result in layer structures of 1-2.5 meter thickness.

Using a geotextile filter is an efficient measure below stone revetments, which can save between 0.3-1.0 m of granular filtermaterial. In addition to these savings, the use of geosynthetics can reduce the CO_2-emissions with appr. 40-50%, due to the significant reduction of the transport of materials. Geosynthetic filter systems in rock revetments have become widely adopted in hydraulic engineering projects, due to their easiness of installation and cost efficiency. Figure 3 gives an example of the construction of a placed block revetment on a nonwoven filter on the slope and rock in the levee toe. For the application it is important to consider the filter and application rules from SBRCURnet (2017) and to ensure adequate robustness to avoid damage by sharp stones as decribed by Bezuijen and Izadi (2018), Izadi et al. (2018), Bezuijen (2023).

Figure 3 – Filter construction using a non-woven geotextile below a placed block revetment on the slope and rock in the levee toe (Markermeerdijken, The Netherlands).

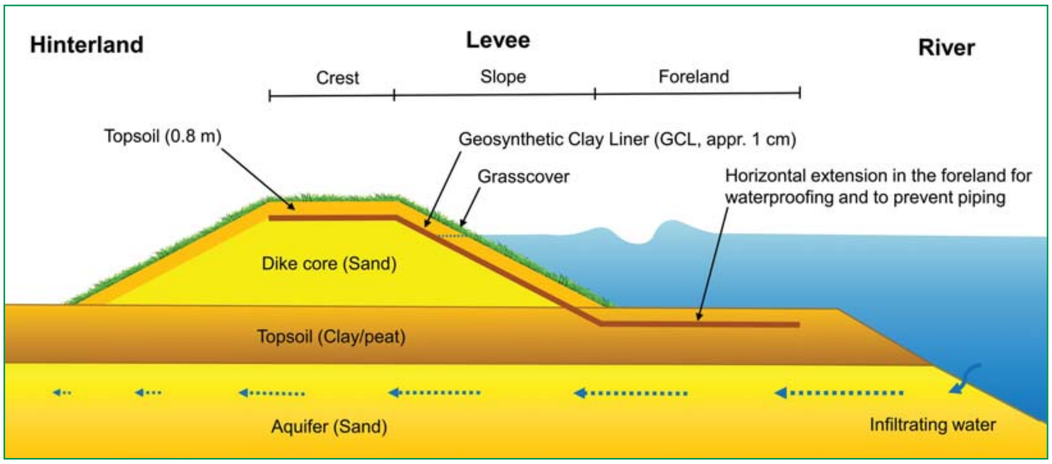

Figure 4 – Geosynthetic Clay Liner (GCL) installed on the levee slope, crest and horizontally in the foreland to enlarge the seepage length from the flood defence base, mitigating the risk of piping.

WATER BARRIERS WITH GEOSYNTHETIC CLAY LINERS (GCLS)

As an alternative for a 1 m thick layer of natural clay, it is possible to implement a Geosynthetic Clay Liner (GCL) in river levees. These mats, with a thickness of approximately 1 cm, consist of a cover and bottom geotextile with high quality bentonite in between. GCLs can be used to seal the foreland as an anti-piping measure, or in the levee itself (Figure 4). Apart from cost savings, Von Mauberge et al. (2022) show that the application of GCLs offers several significant advantages over natural clay such as sustainability (reduced energy requirement and CO_2 emissions for transport), faster construction (less deep excavation and no need for dewatering) and more use of nearby soil. Due to the swelling capacity of the bentonite, the mat is self-healing to a certain extent. In Germany, multiple projects with GCLs in flood defences have been executed in the last decades, for example along the Oder. In the Netherlands, two pilot projects have been initiated by Water Authority Limburg. In Beesel, GCLs have been installed on the crest and slopes of the levee. In Neer, the CGLs were installed in the foreland of the levee to extend the seepage length and prevent piping.

GEOSYNTHETIC SAND CONTAINERS (GSCS) FOR COASTAL PROTECTION AND REDUCING BEACH NOURISHMENT

Sand-filled geotextile containers can be filled on-site and installed on beaches to stabilize the coastline (Figure 5). These containers can also be used in deeper water to prevent scour or to fill up large scour holes. Scouring can occur in riverbeds during floods with extreme discharges, in harbours, or due to hydraulic turbulence around structures like dams and outlet structures.

In the area of Lubmin on the Baltic Sea, a hidden underground protection structure has been built over 2 km of coastline using Geotextile Sand Containers (GSCs). A total of 34,000 sand-filled elements, weighing approximately 1.4 tonnes each, were installed (Figure 6). The structure, being covered with sand seamlessly blends with the coastline, without restrictions for tourism and beach life (Pries, 2022).

Geotextile elements are regularly used as breakwater core, dune foot defence structures, erosion protection or water retaining structures as shown by Pilarczyk (2000) and Bezuijen and Vastenburg (2012). These applications are used world wide. The use of geotextile elements in coastal or flood defence structures has the potential to significantly reduce the risks and effects of beach and dune erosion. This may reduce the number of beach nourishments, costs and maintenance frequency of beaches and dunes after severe storms.

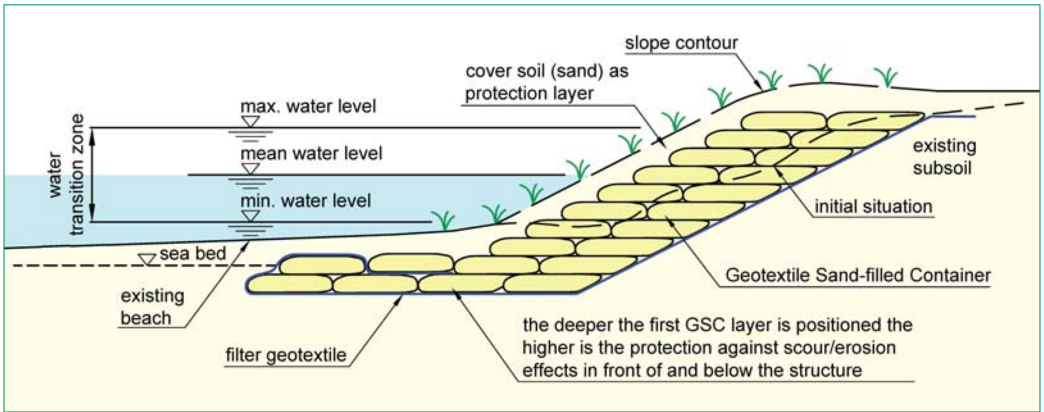

Figure 5 – Schematic cross-section of dune protection using Geotextile Sand Containers (GSCs) underground structure, covered with beach sand and planted with helm grass.

Figure 6 – Installation of Geotextile Sand Containers (GSCs) as a coastal protection measure in the dune core of the sandy beach, Ludmin, Germany.

EROSION PROTECTION WITH 3D STRUCTURE MATS

As a result of climate change, there will be higher water levels, stronger currents, increased waves and heavier rainfall. Therefore, more robust and intelligent erosion protection systems for flood defences are increasingly important. Robust erosion protection is crucial in cases of overflowing levee structures. One effective method of erosion protection is the use of three-dimensional geosynthetic structure mats, which reinforce the topsoil layer on embankments (see Figure 7). These mats, known as High Performance Turf Reinforcement Mats (HPTRMs), provides protection of the bare soil or early vegetation, thus providing extra resistance to erosion. This prevents the washing away of grass seeds or young vegetation, ensuring homogeneous germination, resulting inthe development of a better-quality grass vegetation.

In addition, the structure mats provide a long-lasting reinforcement of the top layer within the root zone. This may be particularly necessary at locations where higher loads are expected, such as breaking waves, overtopping water and strong currents. Special attention should be given to slope transitions, where the loads are often higher and the strength is less.

SOIL REINFORCEMENT FOR EMBANKMENT STABILITY AND STEEP SLOPES

Raising embankments on soft soils can cause stability problems. A regularly applied solution is the installation of high-strength soil reinforcement at the base of the embankment, known as 'basal' reinforcement. The strength of this reinforcement typically ranges from 300 to 1500 kN/m. Along the German-Polish border, along the Oder, a 3 km levee stretch was reconstructed to withstand more extreme flood conditions. In order to ensure sufficient stability of the new levee, a high strength geogrid of 1000 kN/m was installed as a basal foundation reinforcement (Figure 8).

Another application of geosynthetics on flood defences is the realisation of steep slopes to reduce land usage. In many cases, there are existing structures such as houses adjacent to these flood defences. As an alternative to vertical retaining walls of steel or concrete, geogrid reinforced soil structures can be used to create a steep slope, see POV Macrostabiliteit (2018) and CUR/CROW (2018). Retaining walls utilizing geosynthetic reinforcement are generally flexible and are able to deform together with subsoil settlements. This makes geosynthetics highly suitable for reinforcing levees in soft soil areas. By using Finite Element Models (FEM), the relationship between forces, deformation and the interaction between soil and geosynthetics can provide detailed insights.

DRAINAGE SYSTEMS

With the rise of water levels outside the levees and subsidence in the polders, the hydraulic loads on flood defences are increasing. The increased hydraulic head will have a negative effect on the stability of flood defences. However, geosynthetic drainage systems can have a positive effect on hydraulic pressures. Installing levee drainage can be useful to avoid failure mechanisms such as macro and micro stability, by influencing the phreatic water line in the embankment.
Geosynthetic drainage mats consist of 3D structure composites, which must be pressure-stable under the given conditions. These drainage mats can be installed vertically (for example as toe drainage), horizontally (partly under the embankment core or berm) or on the slope.

Figure 7 – Installation of a reinforced High Performance Turf Reinforcement Mat (HPTRM) for slope protection.

Figure 8 – Installation of high strength geogrids as basal reinforcement below the flood defence at the Oder, Germany.

Conclusions

Climate change has significant effects on flood defences world wide. Sea level rise and extreme weather events have consequences for the safety, quality of life and sustainability of residential, industrial and agricultural areas. In the coming decades, extensive and costly operations to flood defences have to be initiated to keep local areas, larger regions or full countries safe and sustainable.

For the challenge of climate adaption, geosynthetics can contribute to adapt safe and resilient living areas for humanity. Geosynthetics can play a positive role in new or existing coastal and riverine flood defence systems: more sustainable, faster and/or cheaper construction. Making future-proof designs with geosynthetics in embankments is also a challenge. Levees must be adaptable to accommodate future levee reinforcements, in which applied geosynthetics in the levee should be manageable and not be an obstacle. Development of integrated concepts with geosynthetics will offer major potentials to advancing flood protection strategies.

References

- Bezuijen, A., Vastenburg, E.W. 2012. Geosystems: design rules and applications, CRC Press.
- Bezuijen A., Izadi E., 2018. Damage of geotextile due to impact of stones, 11th International Conference on Geosynthetic, Seoul, South-Korea.
- Bezuijen A., 2023. Field tests on the impact of stones on geotextile compared with theory, in: proceedings of the 12th International Conference Geosynthetics (12ICG), Roma, Italy.
- CUR/CROW, 2018. Kerende constructies van gewapende grond, CUR-rapport 198, CROW.
- Gerritsen R., Bezuijen, A., Dorst K., 2019. Klimaatverandering en weersextremen: toepassing van geokunststoffen bij waterkeringen en kustverdediging. GeoKunst, GeoTechniek, maart 2019 (deel 1: 46-51) en juni 2019 (deel 2: 48-53).
- Gerritsen R., Bezuijen, A., Dorst K., 2023. Climate change and extreme weather conditions: applications of geosynthetics securing flood defenses and coastal protection, proceedings of the 12th International Conference Geosynthetics (12ICG), Roma, Italy.
- Haasnoot, M., Bouwer, L., Diermanse, F., Kwadijk, J., van der Spek, A., Oude Essink, G., Delsman, J., Weiler, O., Mens, M., ter Maat, J., Huismans, Y., Sloff, K., Mosselman, E. 2018. Mogelijke gevolgen van versnelde zeespiegelstijging voor het Deltaprogramma, een verkenning, Deltares report 11202230-005-0002, Delft.
- IPCC, 2022. Intergovernmental Panel on Climate Change, Technical Summary, IPCC_AR6_WGII_Technical_Summary.pdf.
- Izadi E., Decraene T., De Strijcker S., Bezuijen A., Vinckier D., 2018. A laboratory investigation on the impact resistance of a woven geotextile. Geotextiles and Geomembranes 46 (1), 91-100.
- Jevrejeva, S., Jackson, L.P. Grindsted, A., Linck, D., Marzeion, B., 2018. Flood damage costs under the sea level rise with warming of 1.5 °C and 2 °C, Environmental Research Letters.
- Pilarczyk, K.W., 2000. Geosynthetics and Geosystems in Hydraulic and Coastal Engineering, A.A. Balkema, Rotterdam.
- POV Macrostabiliteit, 2018. POV-M grondverbeteringen, Hoogwater beschermingsprogramma (HWBP), Utrecht. ISBN 978-90-8292 48-0-0.
- Pries, J.K., 2022. Coastal protection with geotextile sand containers at Lubmin in Germany. GeoKunst, GeoTechniek, 72-74.
- SBR CUR net, 2017. Ontwerprichtlijn Geotextielen onder steenbekleding, SBR CUR net, Delft.
- Von Mauberge, K., Gerritsen, R., Ehrenberg, H., 2022. Geosynthetics: responsible and sustainable solutions to reduce environmental impact. GeoKunst, GeoTechniek, 49-56.


B. Wittekoek
Deltares, Delft
Netherlands


S.J.M. van Eekelen
Deltares, Delft
Netherlands


A. Bezuijen
Deltares, Delft
Netherlands


J. Terwindt
Data Engineer at Scarp
DENA, Sweden


O. Detert
Huesker Synthetic
Germany


J.H. van den Berg
Huesker Synthetic
Germany


D. König
Ruhr-Universität Bochum
Germany

GEOGRID-ANCHORED SHEET PILE WALLS UNDER STRIP FOOTING SURCHARGE LOADING, SMALL-SCALE EXPERIMENTS

Introduction

A geogrid-anchored sheet pile wall (SPW) is a relative new application of geogrids (van Duijnen et al., 2022, Wittekoek, 2020, Wittekoek et al., 2022). The system is closely linked to a retaining wall of reinforced soil with a full-height facing as well as to a traditional anchored SPW. However, the geogrid-anchored SPW has more embedment than a retaining wall of reinforced soil. And contrary to a traditionally anchored SPW, a geogrid anchor is also effective within the active soil wedge when the SPW deforms. This paper looks at small scale experiments, to get a feeling for how the system works. This paper is a shorter version of Wittekoek et al. (2023).

Small-scale experiments

Figure 1 shows the test set-up of the small-scale experiments. The aluminium model-SPW models the upper part of the embedded part of the SPW and was free to slide along the box bottom. The polypropylene (PP) model-geogrid had a short-term stiffness of 191 kN/m at 2% axial strain and a short-term tensile strength of 16.2 kN/m at a maximum strain of 13.5%. Table 1 lists the properties of the sand fill.

A silicon block model at the passive side has a stiffness of 159 kPa up to a strain of at least 8%. This silicon block was tailored to simulate passive resistance as realistic as possible. The strip surcharge load is applied by loading a 0.1 m wide footing with a barrel that is filled with water during the test (the blue barrel in Figure 1). The soil-wall friction was minimized with a lubricated thin (< 1mm) transparent silicone sheet. Wittekoek et al. (2022) showed that tests in an eight times wider test box gave similar slip surfaces, proving that the narrow box results were sufficiently reliable to analyse qualitatively. The movement of the soil was tracked using the Particle Image Velocimetry (PIV) technique as implemented by Stanier et al. (2015).

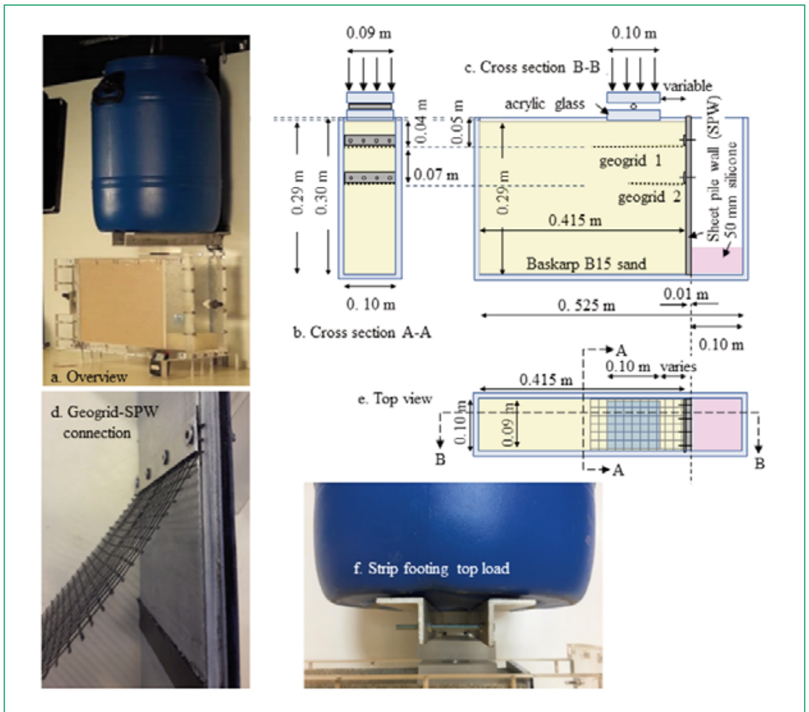

Figure 1 – Test set-up.

Results small-scale experiments

THE LOCATION OF THE STRIP SURCHARGE LOAD

Figure 2 shows how the location of the surcharge load determines the failure mechanism. Two slip surfaces develop from the two edges of the strip footing towards the SPW, dividing the soil into three different zones. Zone I is characterized by rigid soil body motions. The active zone II slides along the critical slip surface 1A. Zone III is stable. The third slip surface in Figure 2 only occurred in Test 19, not in duplicate Test 18 or any other test.

A greater distance between load and SPW results in stiffer behaviour (Figure 3): the wider slip surfaces mobilize more shear resistance, and the load is distributed to deeper soil. Figure 3a and b differ remarkably. If the load is at 84 mm from the SPW, the 60 mm geogrid is located fully in zone I. Nevertheless, the bearing capacity increases compared to the situation without geogrid. The load position has less influence for longer geogrids (Figure 3c and d).

GEOGRID ANCHOR LENGTH

Longer geogrids provide more resistance (Figure 4) which increases the bearing capacity of the entire system. The longest geogrid initially behaves stiffer than the shorter geogrids. Figure 4b shows a straight slip surface for all geogrids.

Table 1 – Properties Baskarp B15 sand.

Parameter	*Value*	*Parameter*	*Value*
Relative density I_D (%)	63-83	Dilatancy angle ψ^{triax} (°)	15.0
Median particle diameter D_{50} (mm)	0.137	Cohesion c (kPa)	0.6
Coefficient of uniformity D_{60}/D_{10} (-)	1.6	Secant Young's modulus at confining pressure of 100 E_{50}^{ref} (MPa)	72.4
Secant internal friction angle φ_{sec}^{triax} (°)	37*	Power in power law material stiffness m (-)	0.54
Residual internal friction angle φ_{res}^{triax} (°)	34	Poisson ratio ν (-)	0.25

* Plane strain value of ($^{11}/_{9}$ • triaxial value =) 45°.

ABSTRACT

Small-scale experiments on geogrid-anchored sheet pile walls (SPWs) under strip footing surcharge loading were conducted at the Deltares laboratory. The following was concluded from the experiments. Two slip surfaces develop, starting at the edges of the strip footing. They divide the soil behind the SPW into three zones. The paper analyses the contributions of each of these zones to the failure load of the structure. The location of the strip footing surcharge load, the geogrid length and the number of geogrid anchors all affect the failure load of the structure. Furthermore, the slip surface reorients at the intersection with geogrids, and even very short geogrid anchors contribute to the total resistance.

Table 2 – The test series. This paper gives results of the tests with bold-printed numbers. Duplicate tests are denoted by a forward slash.

Test number	12/13	14/15	16/17/45	18/19	20/21	22/23	28	30	31	41/42	43/44	47	48	51	52
Number of geogrids	1	1	1	1	2	2	1	1	1	1	1	0	0	1	1
Length geogrids (mm)	110	110	180	180	180+110	180+110	60	60	60	180	110	-	-	130	130
Connected to SPW?	Yes	Yes	Yes	Yes	Yes	Yes	Yes	Yes	No	No	No	-	-	No	Yes
Vertical distance top SPW-geogrid (mm)	50	50	50	50	50+120	50+120	50	50	50	50	50	-	-	50	50
Horizontal distance surcharge load-SPW (mm)	30	60	30	130	130	30	30	84	30	30	30	84	30	30	30
Relative density fill (%)	67/71	73/74	68/74/76	74/73	71/64	74/78	81	78	68	75/76	69/76	75	71	67	65

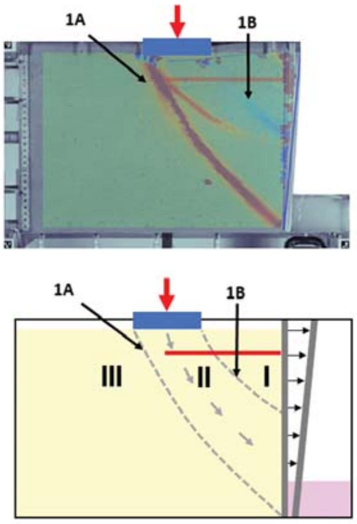

Figure 2 – Slip surfaces for a surcharge load of ~4 kN/m. Test 19. 1A: critical slip surface and 1B: secondary slip surface. The slip surfaces divide the soil in three zones: active zone II between zones I and III.

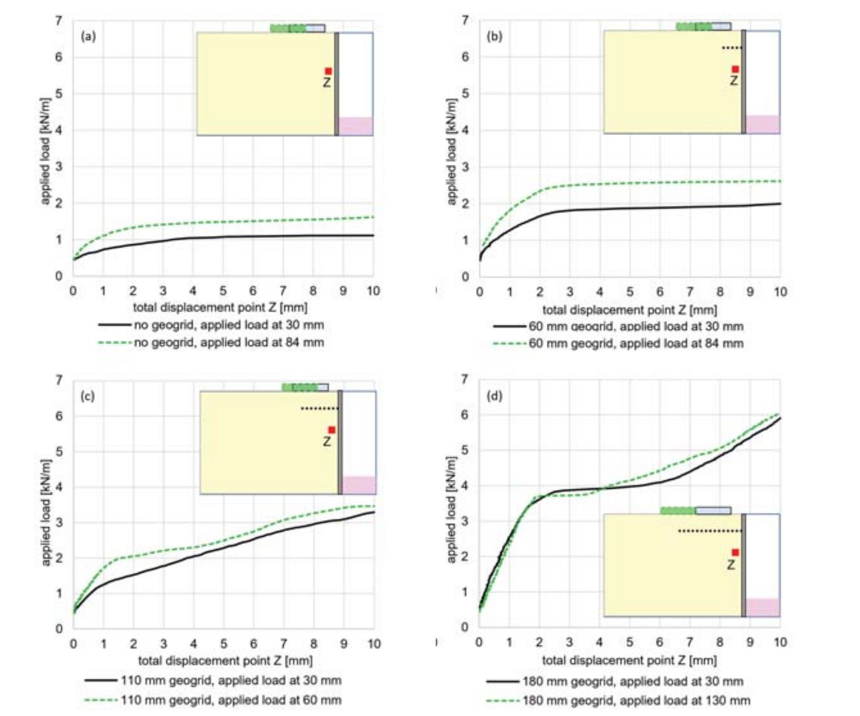

Figure 3 – Influence of the location of the surcharge load (a) without geogrid (b) 60 mm geogrid (c) 110 mm geogrid and (d) 180 mm geogrid.

Only for the longest geogrid of 180 mm (Test 45), the slip surface crosses the geogrid and a second curved slip surface develops. The initial straight slip surface is therefore not the critical one. The geogrid is activated more efficiently, and the orientation of the slip surface at the intersection with the geogrid changes. The geogrid is activated more efficiently, and the orientation of the slip surface at the intersection with the geogrid changes, like also found by Ziegler (2010). The slip surface therefore becomes longer and curved.

A SECOND GEOGRID ANCHOR

Figure 5 compares 1 and 2 geogrids. The deformations are equal up to a surcharge load of 3.0 kN/m. Above 4.0 kN/m, the SPW slides along the box bottom in both tests. This failure mode is triggered by the relatively high resistance of the geogrid anchor(s). For this higher surcharge load, the second geogrid limits the deformations when the vertical pressure on the geogrids (and therefore the soil-geogrid interface friction) increase. This is in line with the 2D FEM calculations of Schoen et al. (2023), that showed that the geogrid anchor is more effective when installed at a lower level.

Contrary to expectations, point Z settles more than point Y. The second geogrid increases this difference. Obviously, the geogrids limit the settlement of the soil above. Figure 6 shows how the second geogrid changes the slip surface: it becomes slightly wider, and therefore longer, as it circumvents the second geogrid.

CONNECTION GEOGRID – SHEET PILE WALL

In four tests, the geogrid was not connected to the SPW (Figure 7). From these tests we conclude that:

– Connecting the geogrid increases the failure load.
– Short non-connected geogrids ≤130 mm hardly contribute to the failure load.
– Short connected geogrids ≤130 mm increase the failure load, although they are located in zones I and II only. So, zones I and II are only activated when the geogrid is connected to the SPW and the geogrid has moved down-

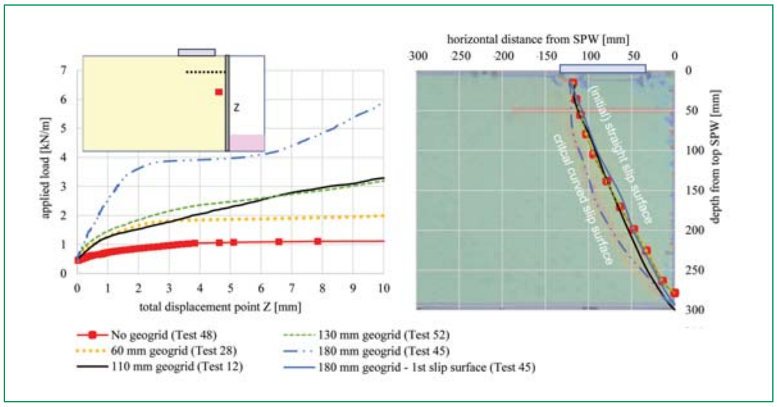

Figure 4 – Influence of the geogrid length. Surcharge load at 30 mm from the SPW. The background of the right-hand figure is Test 45 (180 mm geogrid).

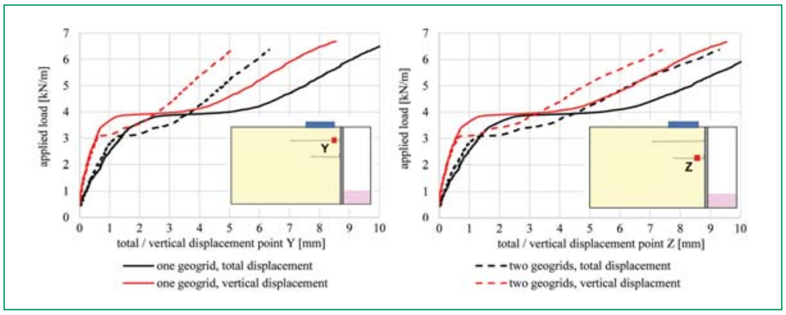

Figure 5 – Load-displacement behaviour for 1 or 2 geogrids. Surcharge load at 30 mm from the SPW. Tests 45 and 22: both have a 180 mm geogrid at the same position, Test 22 has a second geogrid (110 mm).

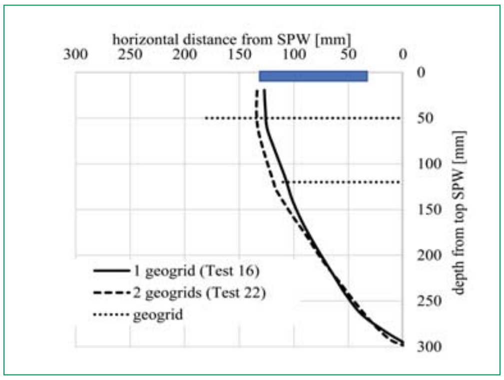

Figure 6 – Slip planes for 1 or 2 geogrids.

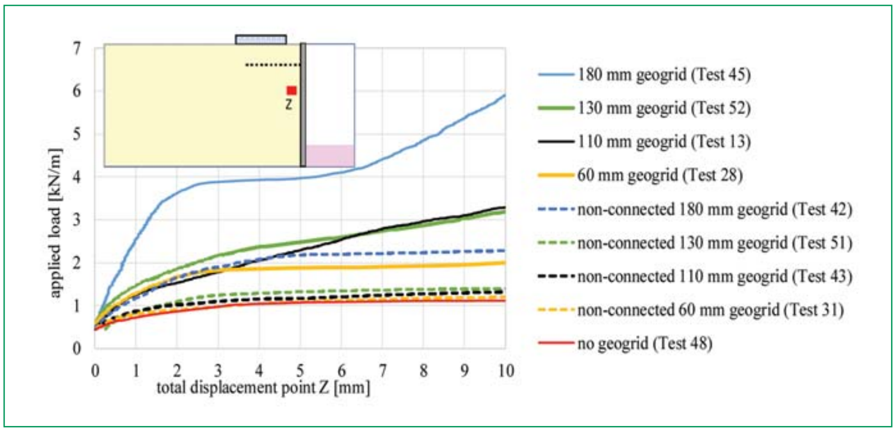

Figure 7 – Difference between geogrids that are connected or not to the SPW.

wards with the soil in zone II.

- Short geogrids ≤130 mm do not reinforce the soil, because the short non-connected geogrids do not provide more failure resistance than found in the situation without geogrid.
- The increase in failure load due to connecting the geogrids (≤130 mm) indicates the presence of the 'membrane effect'. This term refers to the capacity of the geogrid to be deformed, while absorbing forces that were initially perpendicular to its surface. When the geogrid moves downwards with the soil in Zone II, tensile forces develop in the geogrid through which the geogrid transfers vertical soil pressures to zone I, the SPW, if connected, and zone III.
- The 180 mm geogrid, even if not connected to the SPW, contributes to the total resistance. The failure load results from the pull-out resistance in zones I and III.
- Connecting the 180 mm geogrid activates the rear part of the geogrid (zone III) more effectively and increases the failure load. However, the rear part contributes most to the total resistance at higher load levels while the geogrid is being pulled out by the sliding soil mass in zone II.
- The total resistance of a connected geogrid anchor consists of contributions of the membrane effect (zone I), frictional resistance (zone II) and pull-out resistance (zone III).

Conclusions

A series of small-scale tests of geogrid-anchored SPWs led to the following conclusions. Two slip surfaces, starting at the edges of the strip footing, divide the fill behind the SPW into three zones: the active zone II, zone I between SPW and active zone II. The paper analyses the contributions of each of these zones to failure. The location of the strip footing surcharge load, the length of the geogrids and the number of geogrid anchors affect the failure load of the structure. The slip surface at the intersection of the critical slip surface reorients with the geogrids, and even a very short geogrid anchor contributes to the total resistance.

Acknowledgements

The authors are grateful for the support of the TKI-PPS funding of the Dutch Ministry of Economic Affairs, Deltares, Delft University of Technology, GeoTec Solutions, Huesker BV, Huesker GmbH and Ruhr-Universität Bochum Germany.

References

- Schoen, M., König, D., Lavasan, A.A., Wichtmann, T., Hölter, R., Wittekoek, B., van Eekelen, S.J.M., van Duijnen, P.G. & Detert, O. 2023. Numerical investigation of geogrid back-anchored sheet pile walls. In: proc. 12 ICG, Rome, Italy.
- Stanier, S.A., Blaber, J., Take, W.A. and White, D.J. (2015). Improved image-based deformation measurement for geotechnical applications. Canadian Geotechnical Journal. https://doi.org/ 10.1139/cgj-2015-0253.
- van Duijnen, P.G., Detert, O., Lavasan, A.A., van den Berg, J., König, D., Hölger, R., van Eekelen, S.J.M. 2022. Geogrid-anchored sheet pile walls: first trial project. In: proc. Eurogeo7, Warsaw, Poland.
- Wittekoek, B. 2020. Analysis of the behaviour of geogrid-anchored sheet pile walls. Small-scale experiments and 2D Plaxis analysis. MSc thesis TU Delft. https://repository.tudelft.nl/islandora/object/uuid%3A94cf64cc-ff09-4fbe-bde8-42d914 b3c7d0.
- Wittekoek, B., van Eekelen, S.J.M., Terwindt, J., Korff, M., van Duijnen, P.G., Detert, O. and Bezuijen, A. 2022. Geogrid-anchored sheet pile walls; a small-scale experimental and numerical study. Geosynthetics International. https://doi.org/10.1680/jgein.22.00501
- Wittekoek, B., van Eekelen, S.J.M., Bezuijen, A., Terwindt, J., van Duijnen, P.G., Detert, O., van den Berg, J.H., and König, D., 2023. Geogrid-anchored sheet pile walls under strip footing surcharge loading, small-scale experiments. In: proc. 12ICG, Rome, Italy.
- Ziegler, M. 2010. Investigation of the Confining Effect of Geogrid Reinforced Soil with Plane Strain Model Wall Tests. Aachen, Germany: Rheinische Westfälische Technische Hochschule Aachen (RWTH). ●

(Credits: RWE)

Constructing windmills on a sea-defense dike in The Netherlands with Enka Solutions

The Netherlands is a small, densely populated country where space for any type of construction is at a premium. This is particularly true when decisions on the construction of windfarms have to be made, and every effort is made to locate these away from centers of population. The construction of a windfarm in the north of the country is a good example of this.

To make the most of both available space and wind, it was planned to locate the windfarm on a primary sea-defense dike – a world first for this application. The dike was already scheduled for upgrading, and the additional design and construction work required for the foundations and working platforms was readily taken into account in the overall project.

Wind turbines on sea-defense dike

The windfarm Oosterpolderdijk, owned by the energy company RWE, is situated on a primary sea-defense dike in the northeastern tip of the Netherlands, near Eemshaven. The park went into operation at the end of 2021 and consists of three turbines with shaft heights of 98 m. Their construction at a location such as this was a world premiere and was preceded by technical analyses of the dike's hydraulic stability, its robustness, its overall stability, and the risk of a breach.

The sea-defense dike required improvements in both profile and stability. The construction of the windfarm was incorporated in the earthworks involved here, and the windmill foundations were incorporated in the profile of the dike. As the dike protects the lower-lying polders against storm events, floods, and high tides, ensuring hydraulic stability was a top priority both during construction and in the operational phase. This was of course the foremost requirement of the responsible Water Board Noorderzijlvest.

MCHS reinforcement

An additional challenge was the design and construction of the Main Crane Hard Stands (MCHS) and the turbine foundations within the limited working space. Challenged by the contractor, a joint venture of Boskalis and KWS, to come up with a suitable design, the Enka Solutions team proposed a solution including the use of the high-strength bi-axial geogrid Enkagrid MAX 60.

Based on the given parameters and requirements, the team came up with a design summarized as follows:

- Construction of hardstands, 15 x 15 m, next to the three wind turbines
- Application of three Enkagrid MAX 60 geogrid layers embedded in the MCHS structure to increase bearing capacity and stabilization
- Installation of Enkagrid MAX 60 layers at 90° to one another
- Wrap-around methodology used at the toe of the dike to ensure the stability of the platform's steep side slopes

Windfarm Oosterpolderdijk (Credits: RWE)

The use of a climbing construction crane allowed for a smaller hardstand.

Benefits of the solution

The use of Enkagrid MAX 60 in the crane foundation allowed for a significant reduction in layer thickness and weight, while ensuring that crane loads were evenly distributed over the platform structure. The wrap-around method ensures that the structure can withstand the lateral strain at the edges along the steep slope on the landward side of the dike.

About Enkagrid

Enkagrid products include bi-axial and uni-axial geogrids in various tensile strengths. The bi-axial Enkagrid MAX provides the load-uptake capacities needed in the sub-base stabilization of roads, railways and foundations, whereas the uni-axial Enkagrid PRO products are applied in structures such as retaining walls, embankments, or in steep slopes up to 90° to ensure their internal stability.

A special and recently introduced Enkagrid combines the regular bi-axial grid with a nonwoven geotextile in a single product for increased project efficiency. Enkagrid geogrids are made of extruded polymer straps that are laser-welded at regular intervals, guaranteeing high performance and providing excellent interlocking between grid and aggregate.

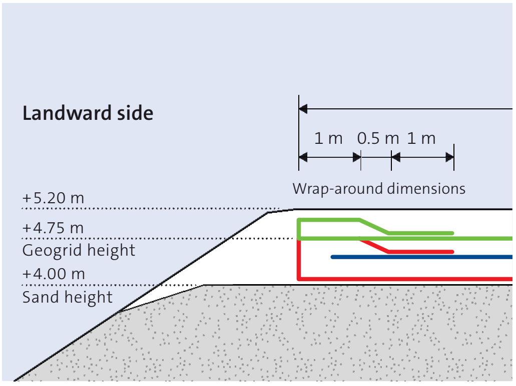

Cross section of the working platform at the embankment toe

Enkagrid® MAX

Enkagrid is a product of Enka Solutions, a global pioneer that introduced the use of geosynthetics to the civil engineering world more than 60 years ago and has been at the forefront of developing many geosynthetic applications ever since. Apart from solutions for soil reinforcement, Enka Solutions products such as Enkamat, Enkadrain and Colbonddrain are used in projects where erosion control, horizontal or vertical drainage, or rapid soil consolidation are required in transportation infrastructure as well as in hydraulic and environmental engineering. A team of experts is ready to support projects from the design phase up to installation. Enka Solutions products are globally available.

Follow Enka Solutions on Linked In for updates on Civil engineering projects and more:

Follow us on LinkedIn

Enka Solutions is a brand of **Freudenberg Performance Materials**

+31 (0)85 744 1300
info@enkasolutions.com
www.enkasolutions.com